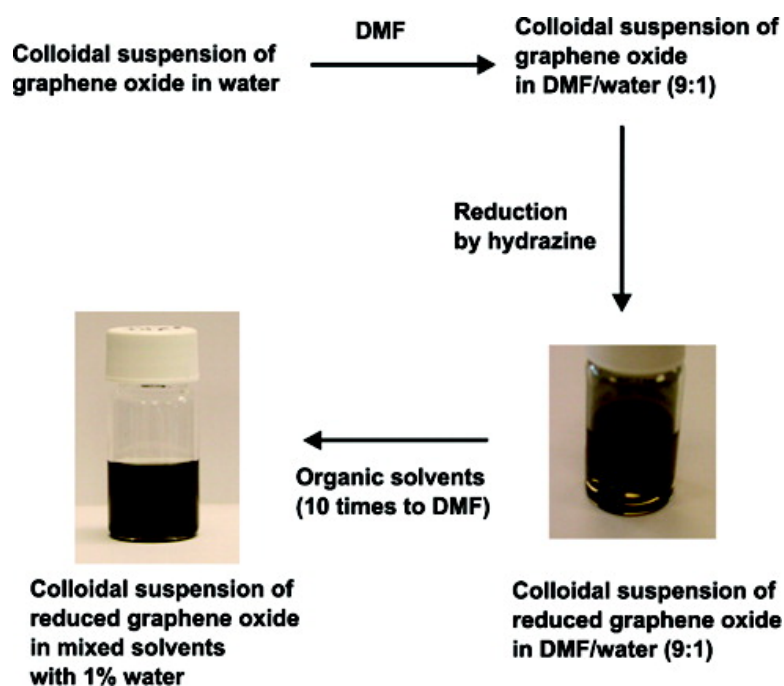


Colloidal Suspensions of Highly Reduced Graphene Oxide in a Wide Variety of Organic Solvents

Sungjin Park, Jinho An, Inhwa Jung, Richard D. Piner, Sung Jin An, Xuesong Li, Aruna Velamakanni, and Rodney S. Ruoff

Nano Lett., 2009, 9 (4), 1593-1597 • DOI: 10.1021/nl803798y • Publication Date (Web): 05 March 2009

Downloaded from <http://pubs.acs.org> on April 8, 2009



More About This Article

Additional resources and features associated with this article are available within the HTML version:

- Supporting Information
- Access to high resolution figures
- Links to articles and content related to this article
- Copyright permission to reproduce figures and/or text from this article

[View the Full Text HTML](#)



ACS Publications
High quality. High impact.

Colloidal Suspensions of Highly Reduced Graphene Oxide in a Wide Variety of Organic Solvents

Sungjin Park, Jinho An, Inhwa Jung, Richard D. Piner, Sung Jin An, Xuesong Li, Aruna Velamakanni, and Rodney S. Ruoff*

Department of Mechanical Engineering and the Texas Materials Institute, The University of Texas at Austin, One University Station C2200, Austin, Texas, 78712-0292

Received December 16, 2008; Revised Manuscript Received February 3, 2009

ABSTRACT

We report that homogeneous colloidal suspensions of chemically modified graphene sheets were readily produced in a wide variety of organic solvent systems. Two different sets of solubility parameters are used to rationalize when stable colloidal suspensions of graphene oxide sheets and, separately, of reduced graphene oxide sheets in a given solvent type are possible and when they are not. As an example of the utility of such colloidal suspensions, “paperlike” materials generated by very simple filtration of the reduced graphene oxide sheets had electrical conductivity values as high as 16 000 S/m.

Graphene-based materials are of interest among other reasons due to the excellent properties that the graphene sheet has.^{1–4} An important challenge involves achieving homogeneous colloidal suspensions of individual graphene sheets by scalable synthesis methods to accelerate the use of such colloidal suspensions, including on large scale. Herein, we report that homogeneous colloidal suspensions of chemically modified graphene sheets (highly reduced graphene oxide, “HRG”) were readily produced in organic solvent systems. Two different sets of solubility parameters are used to rationalize when stable colloidal suspensions of HRG in a given solvent type are possible and when they are not. “Paperlike” materials generated by simple filtration of HRG had electrical conductivity values as high as 16 000 S/m.

Graphite oxide (GO)^{5–17} or graphite derivatives^{18–21} have been used as a starting material in the production of colloidal suspensions of thin platelets. While graphene oxide that is obtained by simple sonication of graphite oxide is electrically insulating, graphene oxides reduced by chemical,^{8,11,14–17,22,23} thermal,^{24,25} and UV-assisted¹⁴ approaches have been shown to be electrically conductive and hold promise in various applications. Graphene sheets are hydrophobic and readily agglomerate in hydrophilic solvents and evidently in solvents that do not have the right range of cohesive energies.²² Consequently, production of a homogeneous colloidal suspension of electrically conductive graphene sheets in solvents

allowing their broad use for both fundamental study and in applications is a significant challenge.

Colloidal suspensions of conducting graphene sheets decorated/coated by surfactants/stabilizers (e.g., polymers, nanoparticles, small molecules, and polar solvents) have been produced.^{7,8,14,15,18,20–22} The generation of well-dispersed graphene sheets in solvents without surfactants or other stabilizers is intrinsically useful. Recently, aqueous colloidal suspensions of conductive chemically modified graphenes without surfactants/stabilizers were demonstrated through chemical modifications of graphene oxide sheets using electrostatic stabilization between negatively charged carboxylate groups at the edges of the reduced graphene oxide sheets,¹¹ by sulfonyl-functionalization of partly reduced graphene oxide and then further reduction,¹⁶ and via reduction of a K⁺ ion-modified graphene oxide.¹³ Achieving a suspension of conductive graphene sheets without surfactants/stabilizers in a wide range of solvents has not been achieved.

We have tried to disperse graphene oxide in *N,N*-dimethylformamide (DMF) at different concentrations (0.1–1 mg graphite oxide (GO)/mL) by sonication of GO⁹ that had been produced by the modified Hummers method.¹³ However, even lengthy sonication (over 24 h) in an ultrasound bath did not produce a homogeneous suspension. Further chemical reduction of the mixture using hydrazine monohydrate resulted in agglomerated powders. To generate a homogeneous colloidal suspension of reduced graphene oxide in organic solvent systems, we first started off with pre-dispersed graphene oxide sheets in water (Figure 1; see the

* To whom correspondence should be addressed. E-mail: r.ruoff@mail.utexas.edu.

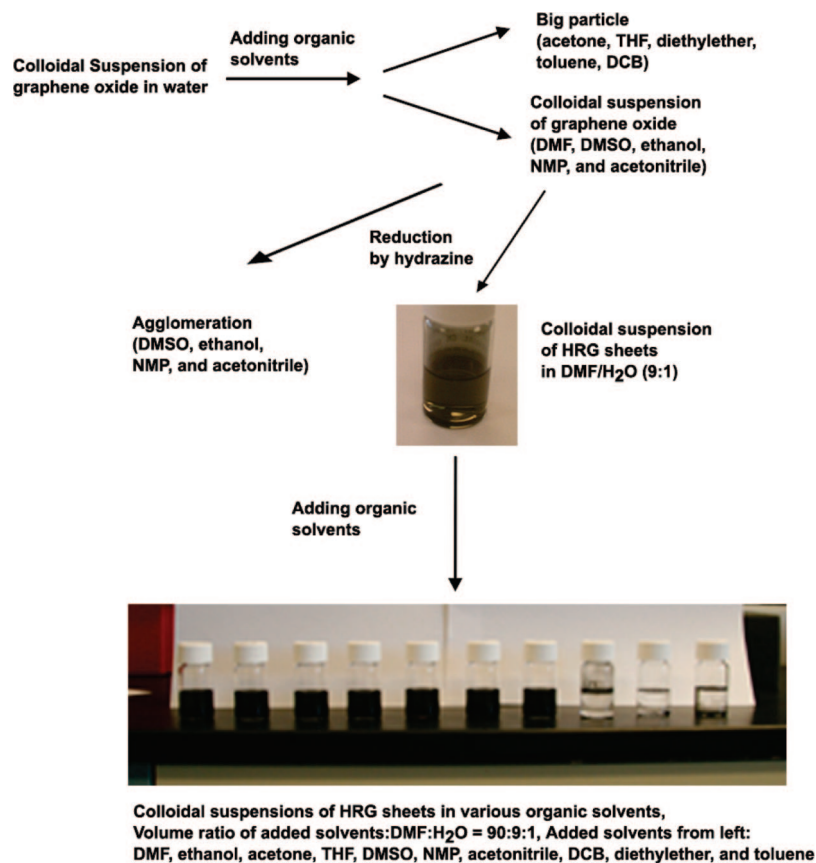


Figure 1. Schematic diagram to produce homogeneous colloidal suspensions of HRG sheets.

methods section of Supporting Information for experimental details). An aqueous graphene oxide suspension (4 mL H₂O, 3 mg GO/mL) was generated by sonication (1 h) of GO. After addition of DMF (volume ratio DMF/H₂O = 9, resulting concentration = 0.3 mg GO/mL), the light-brown suspension of graphene oxide sheets was quite stable. For example, no floating or precipitated particles were observed after 4 months. Chemical reduction of the suspension of graphene oxide sheets was done with hydrazine monohydrate (1 μ L/3 mg GO) for 12 h at 80 °C with stirring by a Teflon-coated magnetic bar, creating a homogeneous black suspension (Figure 1) of HRG sheets with a small number of agglomerated black particles. The resulting suspension was neutral with a pH of \sim 7. The agglomerated particles could be redispersed with a short sonication of less than 5 min. That the HRG is present almost entirely as individual sheets in the DMF/H₂O was confirmed by noncontact mode atomic force microscopy (AFM) and transmission electron microscopy (TEM). Dried-down deposits of HRG sheets on the mica were scanned by AFM using a diluted HRG suspension by adding DMF into the DMF/H₂O (9:1) suspension. On the basis of numerous AFM images, only individual flat HRG sheets with thickness of 0.7 \sim 0.8 nm were observed with lateral dimensions of several hundred nanometers for a single HRG sheet (Figure 2a,b). TEM samples were prepared by dip coating HRG sheets onto a lacey carbon TEM grid in a similarly diluted HRG suspension. As can be seen from a bright field TEM (BF TEM) image in Figure 2c, the sheets are somewhat wrinkled on the grid.

We have tried to generate colloidal suspensions of graphene oxide sheets in other organic solvent systems after first dispersing in water (see Figure 1, organic solvents/H₂O = 9 in volume, tested solvents: *N*-methylpyrrolidone (NMP), ethanol, dimethylsulfoxide (DMSO), acetonitrile, acetone, tetrahydrofuran (THF), diethylether, toluene, and 1,2-dichlorobenzene (DCB)) with the same procedure as described above for DMF. Addition of NMP, ethanol, DMSO, and acetonitrile to an aqueous suspension of graphene oxide produced stable homogeneous colloidal suspensions of the graphene oxide sheets. Adding acetone and THF created suspensions of graphene oxide sheets; however, particles visible to the eye (but not precipitated) were observed after 1 day. The resulting mixtures were readily redispersed by short sonication or stirring and then such particles, again not precipitated, were again seen by the eye after 1 day. Precipitation of agglomerated graphene oxide sheets was immediately observed by the addition of diethylether or toluene to the aqueous suspension. DCB was immiscible with the aqueous suspension and so was not considered. We have reduced the graphene oxide sheets in the successful colloidal suspensions (NMP, ethanol, DMSO, or acetonitrile; each with 9:1 volume ratio to H₂O) by addition of hydrazine monohydrate. Of the other solvent systems that produced a homogeneous suspension of graphene oxide sheets in 9:1 volume ratio with water, none other than DMF had a stable suspension of HRG after addition of the same volume of hydrazine monohydrate, indicating that the reduction in DMF/H₂O seems to be the best system for producing the

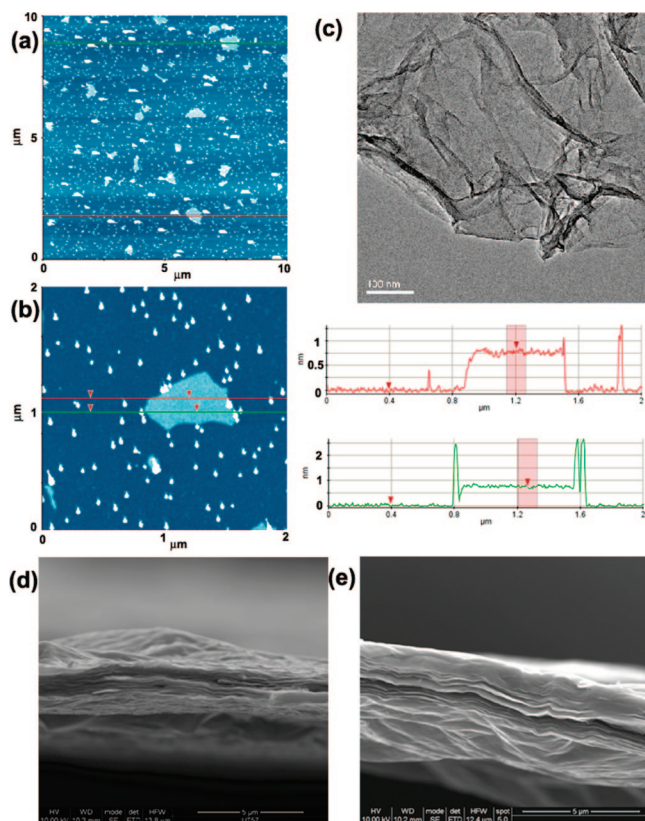


Figure 2. Microscopic images for HRG sheets. (a) An AFM image with 10 μm scale, (b) an AFM image with 2 μm scale, and (c) a TEM image, scale bar = 100 nm; SEM images of the cross-section of (d) the air-dried HRG paper and (e) the HRG paper that had been “dried” at 150 $^{\circ}\text{C}$ under Ar(g).

HRG colloidal suspension (at this 9:1 volume ratio). We have further applied a wide range of organic solvents (DMF, DMSO, THF, NMP, acetonitrile, acetone, ethanol, diethylether, toluene, and DCB) to the aforementioned HRG suspension in DMF/H₂O (9 to 1 volume ratio). Organic solvents were added in 1 mL increments up to a total of 9 mL to 1 mL of the suspension (0.3 mg of starting GO in the suspension of 9 parts DMF in 1 part H₂O) of HRG. Homogeneous colloidal suspensions of HRG were produced at each 1 mL increment up to the final added 9 mL, by the addition of DMF, DMSO, THF, NMP, acetonitrile, acetone, and ethanol (Figure 1). Notably, the resulting suspension (0.3 mg of starting GO/10 mL in mixed solvent; thus, added organic solvent/DMF/H₂O = 90:9:1) contains a small amount of H₂O, about 1% by volume, (e.g., DMSO/DMF/H₂O = 90:9:1, THF/DMF/H₂O = 90:9:1, and DMF/H₂O = 99:1 volume ratio, as examples). However, addition of toluene, diethylether, and DCB to the suspension in DMF/H₂O (9:1) produced black agglomerated powders. To the best of our knowledge, a colloidal suspension of chemically reduced graphene oxide without surfactants/stabilizers in organic solvents has been hereby achieved and reported for the first time.

It is of interest to classify the solvents as to “dispersing power” for HRG based on solubility parameters. We have previously discussed the solubility of fullerenes²⁶ and of single-walled carbon nanotubes²⁷ in terms of solubility

parameters. The Hansen solubility parameters²⁸ include δ_d (dispersion cohesion parameter), δ_p (polarity cohesion parameter), and δ_h (hydrogen bonding cohesion parameter). The values of δ_d , δ_p , and δ_h for the solvents tested are shown in the Supporting Information. The DMF/H₂O mixed solvent further mixed with each of acetone, acetonitrile, THF, DMF, NMP, DMSO, and ethanol and thus having the sum $\delta_p + \delta_h$ in the range of 13~29 showed a good dispersion of HRG. On the other hand, HRG was not dispersed in solvents with $\delta_p + \delta_h$ less than 10 (DCB, diethylether, and toluene) or much higher than 30 (water); see Supporting Information for details. To test whether the solubility parameters could then be used to predict whether some untested solvents would form good colloidal suspensions or not, three different classes of solvents were chosen having $\delta_p + \delta_h$ values: (i) below 10 (chloroform, 8.8 and benzene, 2.0), (ii) over 30 (methanol, 34.6), and (iii) between 13 and 29 (pyridine, 14.7 and propylene carbonate (PC), 22.1). While addition of 9 mL of chloroform, benzene, or methanol to a 1 mL suspension of HRG in DMF/H₂O (9:1 volume ratio) yielded agglomerates, the addition of 9 mL of pyridine or PC generated homogeneous suspensions of HRG. Although we have not exhaustively tested all solvents, the classification using the Hansen solubility parameters should provide an extremely valuable method for predicting which solvents and mixtures of solvents will work well in this regard. The Supporting Information includes results and discussion of suspension (or lack thereof) of graphene oxide sheets and classification based on the Hansen solubility parameters as well as the use of another set of solubility parameters, Taft and Kamlet’s scales,^{29,30} for evaluating suspension (or lack thereof) of either graphene oxide sheets or HRG sheets.

Shiny black and compliant paper samples^{11,13,15,31–33} were fabricated by filtration of the HRG suspension in DMF/H₂O (9:1) using an Anodisc membrane filter (47 mm diameter, 0.2 μm pore size, Whatman, Middlesex, UK) and the HRG paper samples were then dried in air. A scanning electron microscopy (SEM) image of the cross-section of such an air-dried HRG paper sample (fractured by tweezers at room temperature) exhibited a layered structure of HRG sheets (Figure 2d). The Raman spectra of the HRG paper samples showed two broad peaks, a D band at 1344 cm^{-1} and a G band at 1590 cm^{-1} (see Supporting Information for Raman spectra and XRD data).³⁴ XRD of the graphene oxide paper shows a distinct peak at 11.10 $^{\circ}$ corresponding to a d-spacing (in this case, an interlayer distance between sheets) of approximately 7.96 \AA that is due to interlamellar water trapped between hydrophilic graphene oxide sheets.^{31,32,35,36} On the other hand, the peak at 11.10 $^{\circ}$ in the XRD spectrum of air-dried HRG paper is not present and a broad peak was observed at around 23 $^{\circ}$ (3.86 \AA) close to but certainly larger than the d_{002} -spacing of graphite (3.35 \AA). The electrical resistance of air-dried HRG paper samples was measured by the Van der Pauw method, and an average value for the electrical conductivity of $1.69 \pm 0.02 \times 10^3$ S/m was obtained (from three samples). In an attempt to remove residual DMF (boiling point = \sim 152 $^{\circ}\text{C}$) and/or H₂O trapped in the air-dried HRG paper, it was dried at \sim 150 $^{\circ}\text{C}$ for

Table 1. Electrical Conductivities of Free-standing Paper Samples of Modified Graphenes

reduced graphene oxide	drying temperature	conductivity (S/m)
HRG	air	1700
	at 150 °C	16000
reduced graphene oxide at basic condition ^{11,33}	air	7200
	at 220 °C	11800
	at 500 °C	35100
reduced K-modified graphene oxide ¹³	air	690
pyrene derivative-adsorbed reduced graphene oxide ¹⁵	air	200

12 h in a tube furnace under a flow of Ar (see the Methods section of Supporting Information); the layered structure of HRG sheets was maintained as confirmed by SEM images of the cross-section of the fractured sample at room temperature (Figure 2e). The XRD of the HRG paper dried in this way at 150 °C has a sharper peak with a slight shift in the peak maximum to 24° (approximately 3.70 Å). This shift in the interlayer spacing might be attributed to the reduction of the graphene oxide sheets, where the reduction allows the reduced graphene oxide sheets to pack tighter (smaller interlayer distance between sheets) than the less-reduced counterpart. The electrical conductivity ($1.64 \pm 0.10 \times 10^4$ S/m; average of three samples) dried in this way at 150 °C was ~9 times higher than that of the samples that were air-dried at room temperature. On the basis of a comparison with conductivity values reported previously of paper materials composed of chemically modified graphene sheets, our HRG paper samples had higher electrical conductivity (Table 1) with the exception of samples heat-treated at 500 °C.

On the basis of thermal gravimetric analysis (TGA) under air flow (heating rate = 1 °C/min), a TGA curve of air-dried graphene oxide paper sample showed significant weight loss (10~20 wt %) before 100 °C,^{13,22} likely due to evaporation of water molecules that are contained in the material. A TGA curve (see Supporting Information) of the air-dried HRG paper sample showed no mass loss up to 180 °C, indicating that almost no water molecules are trapped in such paperlike samples and thus that the HRG material is hydrophobic—and also not hygroscopic. The TGA curve of the HRG paper sample further showed that the sample lost a small mass (~4 wt %) from 180 to 260 °C and then lost a significant mass (~16 wt %) from 260 to 280 °C, possibly due to evaporation of trapped DMF and/or loss of CO and CO₂ from decomposition of labile oxygen functional groups;³⁷ TGA with mass spectrometry readout of evolving gaseous products is indicated for future study. After further drying (at 150 °C under Ar(g)) the air-dried HRG paper, we measured the mass loss (~27 wt %) with a balance, which is similar but not identical to the accumulated mass loss measured by TGA from room temperature to 280 °C (~20 wt %). Elemental analysis by combustion of paper samples showed an increased C/O atomic ratio in air-dried HRG (11.0) relative to that in the sample composed of graphene oxide platelets (1.2; this value includes contributions from adsorbed water molecules). The C/O atomic ratio (11.0) of air-dried HRG paper is slightly higher than those of ag-

glomerated chemically reduced graphene oxide (10.1; reduction with hydrazine²²) or thermally exfoliated graphite oxide (10.3)²⁵ obtained by expansion of GO through thermal shock. Nitrogen (~3.8 wt %) was found in the air-dried HRG paper and can be attributed to N bonded to graphene by hydrazine reduction, and/or perhaps also from residual DMF (C₃H₇NO) and/or hydrazine (N₂H₄). The C/N atomic ratio (25.7) of the air-dried HRG paper is higher than that found for chemically reduced graphene oxide generated from an aqueous system in which DMF is not used (16.1).²²

Reduction of oxygen functional groups in HRG was also confirmed by X-ray photoelectron spectroscopy (XPS) of paper samples of graphene oxide and, separately, of HRG. Graphene oxide contains a wide range of oxygen functional groups such as hydroxyl, epoxide, carboxyl, and carbonyl groups.^{37–39} In comparison to the C1s spectrum of the graphene oxide paper, peak(s) assigned to oxygen-containing functional groups^{13,32,34} in the HRG paper were significantly decreased after reduction (see Supporting Information). A small peak remains adjacent to the large peak attributed to the C=C bond; this might be due to C–N bonding and/or nonreduced oxygenated carbon. The XPS spectrum of the HRG papers had a small N1s component (that is not observed in the graphene oxide paper) at ~400 eV corresponding to the C–N bond.³⁴ A peak is not observed at ~398 eV (assigned to N–N)³⁴ meaning that if residual hydrazine (NH₂–NH₂) is present, it is below the detection limit of XPS, which probes the surface of such samples. In comparison to the Fourier transformed infrared spectroscopy (FT-IR) spectrum of graphene oxide paper, peaks due to oxygen functional groups are almost entirely removed in the HRG paper sample (see Supporting Information).³²

This approach for dispersing graphenelike sheets in various organic solvents without the use of surfactants/stabilizers and the clarification of dispersibility based on solubility parameters should be extremely useful for the production of a very wide range of colloidal suspensions for fundamental study, and for their use in a wide variety of applications including in the fabrication of polymer-based composites and thin films.

Acknowledgment. This work was supported by a startup package to R.S.R. by The University of Texas at Austin and by the Texas Nanotechnology Research Superiority Initiative (TNRSI)/SWAN.

Supporting Information Available: This includes experimental details, a discussion about prediction for dispersion, XRD, XPS, FT-IR, and Raman data. This material is available free of charge via the Internet at <http://pubs.acs.org>.

References

- (1) Geim, A. K.; Novoselov, K. S. *Nat. Mater.* **2007**, *6*, 183–191.
- (2) Lee, C.; Wei, X.; Kysar, J. W.; Hone, J. *Science* **2008**, *321*, 385–388.
- (3) Zhang, Y.; Tan, Y.-W.; Stormer, H. L.; Kim, P. *Nature* **2005**, *438*, 201–204.
- (4) Balandin, A. A.; Ghosh, S.; Bao, W.; Calizo, I.; Teweldebrhan, D.; Miao, F.; Lau, C. N. *Nano Lett.* **2008**, *8*, 902–907.
- (5) Stankovich, S.; Piner, R.; Nguyen, S. T.; Ruoff, R. S. *Carbon* **2006**, *44*, 3342–3347.
- (6) Niyogi, S.; Bekyarova, E.; Itkis, M. E.; L., M. J.; Hamon, M. A.; Haddon, R. C. *J. Am. Chem. Soc.* **2006**, *128*, 7720–7721.

- (7) Stankovich, S.; Piner, R.; Chen, X.; Wu, N.; Nguyen, S. T.; Ruoff, R. S. *J. Mater. Chem.* **2006**, *16*, 155–158.
- (8) Muszynski, R.; Seger, B.; Kamat, P. V. *J. Phys. Chem. C* **2008**, *112*, 5263–5266.
- (9) Paredes, J. I.; Villar-Rodil, S.; Martinez-Alonso, A.; Tascon, J. M. D. *Langmuir* **2008**, *24*, 10560–10564.
- (10) Ramanathan, T.; Abdala, A. A.; Stankovich, S.; Dikin, D. A.; Herrera-Alonso, M.; Piner, R. D.; Adamson, D. H.; Schniepp, H. C.; Chen, X.; Ruoff, R. S.; Nguyen, S. T.; Aksay, I. A.; Prud'homme, R. K.; Brinson, L. C. *Nat. Nanotechnol.* **2008**, *3*, 327–331.
- (11) Li, D.; Muller, M. B.; Gilje, S.; Kaner, R. B.; Wallace, G. G. *Nat. Nanotechnol.* **2008**, *3*, 101–105.
- (12) Stankovich, S.; Dikin, D. A.; Dommett, G. H. B.; Kohlhaas, K. M.; J., Z. E.; Stach, E. A.; Piner, R.; Nguyen, S. T.; Ruoff, R. S. *Nature* **2006**, *442*, 282–286.
- (13) Park, S.; An, J.; Piner, R. D.; Jung, I.; Yang, D.; Velamakanni, A.; Nguyen, S. T.; Ruoff, R. S. *Chem. Mater.* **2008**, *20*, 6592–6594.
- (14) Williams, G.; Serger, B.; Kamat, P. V. *ACS Nano* **2008**, *2*, 1487–1491.
- (15) Xu, Y.; Bai, H.; Lu, G.; Li, C.; Shi, G. *J. Am. Chem. Soc.* **2008**, *130*, 5856–5857.
- (16) Si, Y.; Samulski, E. T. *Nano Lett.* **2008**, *8*.
- (17) Tung, V. C.; Allen, M. J.; Yang, Y.; Kaner, R. B. *Nat. Nanotechnol.* **2009**, *4*, 25–29.
- (18) Li, X.; Wang, X.; Zhang, L.; Lee, S.; Dai, H. *Science* **2008**, *319*, 1229–1232.
- (19) Liu, N.; Luo, F.; Wu, H.; Liu, Y.; Zhang, C.; Chen, J. *Adv. Funct. Mater.* **2008**, *18*, 1518–1525.
- (20) Li, X.; Zhang, G.; Bai, X.; Sun, X.; Wang, X.; Wang, E.; Dai, H. *Nat. Nanotechnol.* **2008**, *3*, 538–542.
- (21) Hernandez, Y.; Nicolosi, V.; Lotya, M.; Blighe, F. M.; Sun, Z.; De, S.; McGovern, I. T.; Holland, B.; Byrne, M.; K., G. K. Y.; Boland, J. J.; Niraj, P.; Duesberg, G.; Krishnamurthy, S.; Goodhue, R.; Hutchison, J.; Scardaci, V.; Ferrari, A. C.; Coleman, J. N. *Nat. Nanotechnol.* **2008**, *3*, 563–568.
- (22) Stankovich, S.; Dikin, D. A.; Piner, R.; Kohlhaas, K. M.; Kleinhammes, A.; Jia, Y.; Wu, Y.; Nguyen, S. T.; Ruoff, R. S. *Carbon* **2007**, *45*, 1558–1565.
- (23) Wang, G.; Yang, J.; Park, J.; Wang, B.; Liu, H.; Yao, J. *J. Phys. Chem. C* **2008**, *112*, 8192–8195.
- (24) McAllister, M. J.; Li, J.-L.; Adamson, D. H.; Schniepp, H. C.; Abdala, A. A.; Liu, J.; Herrera-Alonso, M.; Milius, D. L.; Car, R.; Prud'homme, R. K.; Aksay, I. A. *Chem. Mater.* **2007**, *19*, 4396–4404.
- (25) Schniepp, H. C.; Li, J.-L.; McAllister, M. J.; Sai, H.; Herrera-Alonso, M.; Adamson, D. H.; Prud'homme, R. K.; Car, R.; Saville, D. A.; Aksay, I. A. *J. Phys. Chem. B* **2006**, *110*, 8535–8539.
- (26) Ruoff, R. S.; Tse, D. S.; Malhotra, R.; Lorents, D. C. *J. Phys. Chem.* **1993**, *97*, 3379–3383.
- (27) Ausman, K. D.; Piner, R.; Lourie, O.; Ruoff, R. S. *J. Phys. Chem. B* **2000**, *104*, 8911–8915.
- (28) Hansen, C. M. *Hansen Solubility Parameters: A User's Handbook*; 2nd ed.; CRC Press: Hoboken, 2007.
- (29) Taft, R. W.; Kamlet, M. J. *J. Am. Chem. Soc.* **1976**, *98*, 2886–2894.
- (30) Marcus, Y. *J. Sol. Chem.* **1991**, *20*, 929–944.
- (31) Dikin, D. A.; Stankovich, S.; Zimney, E. J.; Piner, R.; Dommett, G. H. B.; Evmenenko, G.; Nguyen, S. T.; Ruoff, R. S. *Nature* **2007**, *448*, 457–460.
- (32) Park, S.; Lee, K.-S.; Bozoklu, G.; Cai, W.; Nguyen, S. T.; Ruoff, R. S. *ACS Nano* **2008**, *2*, 572–578.
- (33) Chen, H.; Muller, M. B.; Gilmore, K. J.; Wallace, G. G.; Li, D. *Adv. Mater.* **2008**, *20*, 3557–3561.
- (34) Yang, D.; Velamakanni, A.; Bozoklu, G.; Park, S.; Piner, R. D.; Stankovich, S.; Jung, I.; Field, D. A.; Ventrice, J. C. A.; Ruoff, R. S. *Carbon* **2009**, *47*, 145–152.
- (35) Buchsteiner, A.; Lerf, A.; Pieper, J. *J. Phys. Chem. B* **2006**, *110*, 22328–22338.
- (36) Lerf, A.; Buchsteiner, A.; Pieper, J.; Schottl, S.; Dekany, I.; Szabo, T.; Boehm, H. P. *J. Phys. Chem. Solids* **2006**, *67*, 1106–1110.
- (37) Lerf, A.; He, H.; Forster, M.; Klinowski, J. *J. Phys. Chem. B* **1998**, *102*, 4477–4482.
- (38) Cai, W.; Piner, R. D.; Stadermann, F. J.; Park, S.; Shaibat, M. A.; Ishii, Y.; Yang, D.; Velamakanni, A.; An, S. J.; Stoller, M.; An, J.; Chen, D.; Ruoff, R. S. *Science* **2008**, *321*, 1815–1817.
- (39) He, H.; Riedl, T.; Lerf, A.; Klinowski, J. *J. Phys. Chem.* **1996**, *100*, 19954–19958.

NL803798Y